OPEN-CODE, REAL-TIME EMULATION TESTBED OF GRID-CONNECTED TYPE-3 WIND TURBINE SYSTEM WITH HARDWARE VALIDATION

Maximiliano Ferrari
University of Tennessee
Knoxville, Tennessee, USA
mferrari@vols.utk.edu

Michael Orendorff
NextEra Energy
Juno Beach, Florida, USA
michael.orendorff@fpl.com

Travis Smith
Oak Ridge National Laboratory
Oak Ridge, Tennessee, USA
smithtm@ornl.gov

Mark A. Buckner
Oak Ridge National Laboratory
Oak Ridge, Tennessee, USA
bucknerma@ornl.gov

***Abstract*— This paper presents the design and development of an open-code Type-3 wind turbine virtual-testbed for real-time simulations. The proposed testbed includes the bare code for all the models required to emulate a Type-3 wind turbine system: the Doubly-Fed Induction Generator (DFIG) dynamic model, single-mass drive train, wind turbine system, and average model of the back to back power. This testbed can be executed in PC-layer for offline simulations or can be executed in real-time on the National Instruments (NI)-CompactRIO (cRIO) platform. The discrete-time models are implemented on the Field Programmable Gate Array (FPGA), using LabVIEW, and validated against a physical hardware setup. The emulated stator and rotor currents and DC-link voltage are compared against physical measurements creating a validated platform independent from third-party models and suitable for applications in real-time. The proposed testbed is intended to be available to researchers, wind turbine manufacturers, and utility companies to perform tests using a validated platform to verify proposed control designs of DFIG wind turbines.**

Keywords—doubly-fed induction generator (DFIG), real time simulation, Type-3

NOMENCLATURE

$\boldsymbol{V_s, I_s}$	Stator voltage and current
$\boldsymbol{V_r, I_r}$	Rotor voltage and current
$\boldsymbol{V_f, I_f}$	GSC voltage and current
$\boldsymbol{V_g, I_g}$	Grid voltage and current
$\boldsymbol{\psi_r, \psi_s}$	Stator and rotor flux linkage
$\boldsymbol{d_{abcr}, d_{abcf}}$	Duty cycle rotor and GSC
$\boldsymbol{\omega_m, \omega_s, s}$	Stator, rotor frequency and slip
$\boldsymbol{L_s, L_r}$	Stator and rotor self-inductances
$\boldsymbol{L_m}$	Mutual inductance
$\boldsymbol{L_f}$	GSC inductance
$\boldsymbol{\sigma}$	Leakage coefficient
$\boldsymbol{r_s, r_r, r_f}$	Stator, rotor a grid filter resistance
$\boldsymbol{V_{DC}, I_{DC}}$	DC-link voltage and current
$\boldsymbol{p, J}$	Pole pairs and the inertia
$\boldsymbol{T_m}$	Mechanical torque
$\boldsymbol{T_{EM}}$	Electromagnetic torque

Subscripts

$\boldsymbol{\alpha\beta\gamma}$	Stationary αβγ axis
$\boldsymbol{dq}$	Synchronous dq axis

I. INTRODUCTION

For complex systems like the DFIG it is usually not possible to test and verify control algorithms directly on the physical system due to cost and safety concerns. One alternative to a physical implementation is to design and verify control strategies using real-time simulators, which are a complementary tool to offline simulators, such as Matlab Simulink, PSIM etc.

Review of literature shows that real-time emulation of power electronics and electric machinery have been addressed widely [2]-[5]. Regarding real-time emulation of variable speed wind turbine systems. Authors in [4] present the real-time power-hardware-in-the-loop of the DFIG and the permanent-magnet synchronous machine wind turbine. Authors in [3] implement the DFIG wind turbine on a FPGA board, while in [5] a the DFIG is deployed on a cluster of digital signal processor. However, at the best knowledge of the authors, these research papers do not validate the models against a physical machine or use proprietary hardware to execute the models.

This paper presents the design and development of a open-code grid-connected Type-3 testbed for real-time simulations, presented in seven sections. The real-time models are first developed in sections II-V; and include the DFIG dynamic model, back to back inverter model, mechanical model, and aerodynamic model. Section VI addresses the control design for the back to back converters. The controllers and all the model are implemented on a single NI cRIO 9039 FPGA. Section VII presents the model validation against a physical DFIG setup, which provides a realistic test environment. The physical testbed includes a 250W DFIG, a four-quadrant vector controlled back-to-back power converter, and a PM driver used to emulate the wind, aerodynamic system, and the drive train. The hardware validation is an important step towards revealing the limits in which the DFIG and power converter models are valid. Lastly, section VIII shows how the validated real-time simulator also provides increased performance over offline simulators.

The presented Type-3 testbed can be used to study fault conditions in a safe environment, and to calculate the Proportional-Integral (PI) controllers offline before hardware implementation. Furthermore, the proposed testbed is intended to be available to researchers, wind turbine manufacturers, and utility companies to perform tests in a validated platform to verify proposed control designs of DFIG based wind turbines.

ACKNOWLEDGEMENT Research sponsored by the Laboratory Directed Research and Development Program of Oak Ridge National Laboratory, P.O. Box 2008, Oak Ridge, Tennessee 37831-6285; managed by UT Battelle, LLC, for the U.S. Department of Energy. This manuscript has been authored by UT-Battelle, LLC, under contract DE-AC05-00OR22725 for the U.S. Department of Energy. The United States Government retains and the publisher, by accepting the article for publication, acknowledges that the United States Government retains non-exclusive, paid-up, irrevocable, worldwide license to publish or reproduce the published form of this manuscript, or allow others to do so, for United States Government purposes.

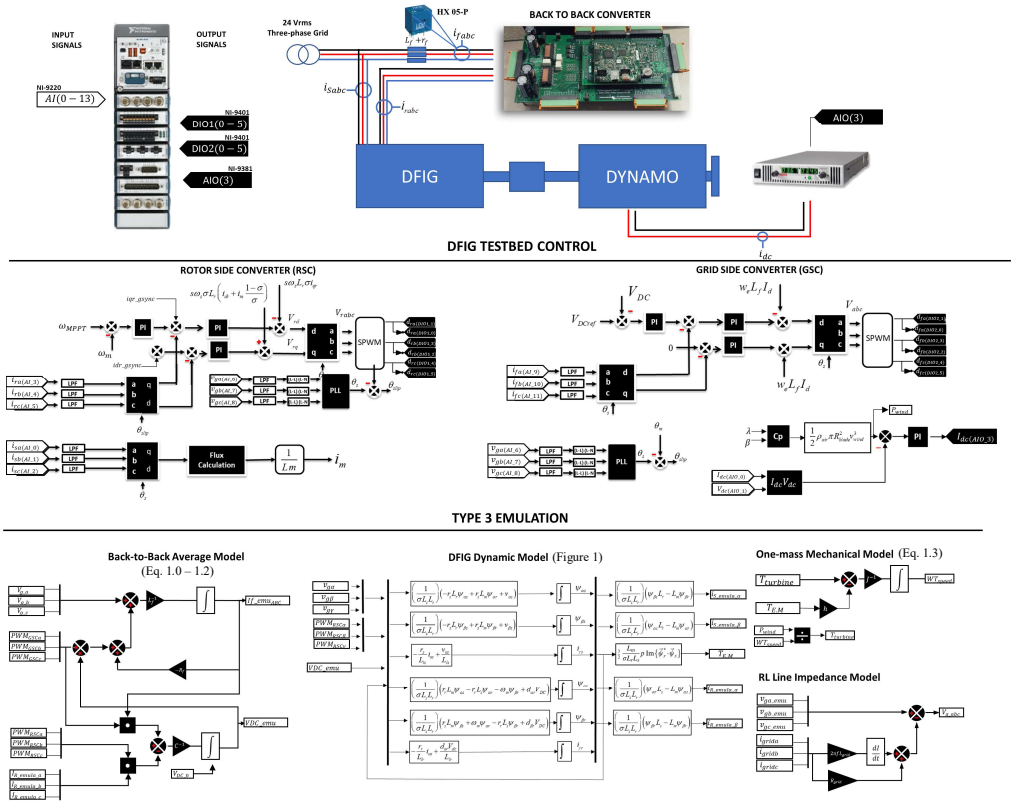

Figure 3: Control Block Diagram for Doubly Fed Induction Generator.

II. DFIG DYNAMIC MODEL

The DFIG dynamic model describes the behavior of the machine in steady state as well the evolution of the electric variables during transients [1]. The dynamic model is computationally intensive because it uses integrators and reference frame transformations that require large space on the FPGA. Since the logic resources on the FPGA are limited, it becomes crucial to find a machine model that uses the fewest resources as possible while providing an accurate representation of the machine dynamics. Review of literature shows four different reference frames that are used to express the electrical variables of the DFIG [9][12][14][15]: The αβγ oriented with either stator or rotor angles, synchronous (dqo), or the natural frame. These models can be represented in matrix form using currents or fluxes as state variables.

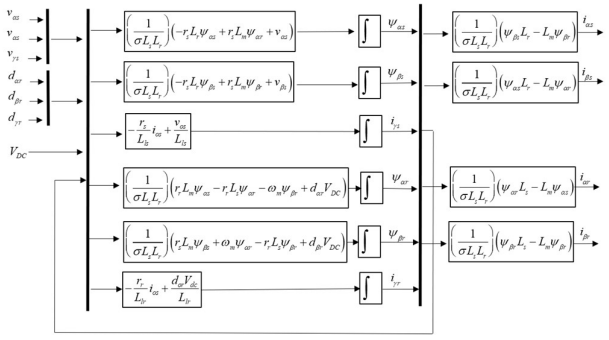

Figure 1: Computer implementation of the rotor oriented DFIG model using fluxes as state-space magnitudes.

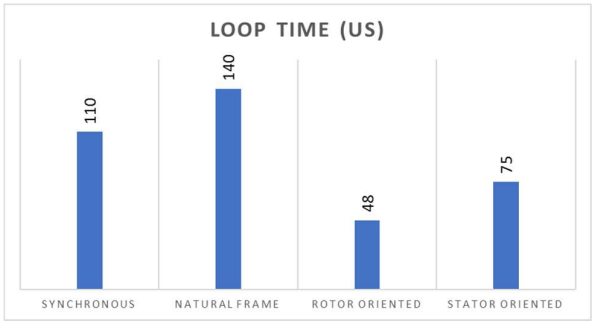

Figure 2: Execution time in microseconds for different models [9].

A previous study showed the state-variable representation and the reference frame impact the model execution time on the FPGA, shown in Figure 2 [9]. For this paper, the αβγ reference frame oriented with respect to rotor angle and using the fluxes as state variables was chosen because its execution time is lower. This efficient machine model enables to emulate the complete Type-3 wind turbine system on a single FPGA.

III. BACK TO BACK MODEL

The back-to-back model consists of the Grid Side Converter (GSC) and the Rotor Side Converter (RSC). Applying Kirchhoff's law and choosing currents as state-variables, the GSC is represented by eq (1.0), the RSC by (1.1) and the DC-link circuit by (1.2):

$$\frac{d}{dt}\begin{bmatrix} i_{af} \\ i_{bf} \\ i_{cf} \end{bmatrix} = -\frac{r_f}{L_f}\begin{bmatrix} i_{af} \\ i_{bf} \\ i_{cf} \end{bmatrix} - \frac{1}{L_f}\begin{bmatrix} v_{ag} \\ v_{bg} \\ v_{cg} \end{bmatrix} - \frac{1}{L_f}\begin{bmatrix} v_n \\ v_n \\ v_n \end{bmatrix} + \frac{v_{DC}}{L_f}\begin{bmatrix} d_{af} \\ d_{bf} \\ d_{cf} \end{bmatrix} \quad (1.0)$$

$$\frac{d}{dt}\begin{bmatrix} i_{ar} \\ i_{br} \\ i_{cr} \end{bmatrix} = -\frac{r_r}{L_r}\begin{bmatrix} i_{ar} \\ i_{br} \\ i_{cr} \end{bmatrix} + \frac{1}{L_r}\begin{bmatrix} e_a \\ e_b \\ e_c \end{bmatrix} + \frac{1}{L_r}\begin{bmatrix} v_n \\ v_n \\ v_n \end{bmatrix} - \frac{v_{DC}}{L_r}\begin{bmatrix} d_{ar} \\ d_{br} \\ d_{cr} \end{bmatrix} \quad (1.1)$$

$$\frac{d}{dt}V_{DC} = \frac{1}{C}\left[\begin{bmatrix} d_{ar} & d_{br} & d_{cr} \end{bmatrix}\begin{bmatrix} i_{ar} \\ i_{br} \\ i_{cr} \end{bmatrix} - \begin{bmatrix} d_{af} & d_{bf} & d_{cf} \end{bmatrix}\begin{bmatrix} i_{af} \\ i_{bf} \\ i_{cf} \end{bmatrix}\right] \quad (1.2)$$

IV. MECHANICAL MODEL

Assuming a perfect rigid low speed shaft, the two-mass train model is reduced to a one-mass drive train model. The resulting governing equation is [10]:

$$\frac{d\omega_m}{dt} = \frac{p}{J}(T_m - T_{EM}) \quad (1.3)$$

V. AERODYNAMIC MODEL

The amount of power that could be extracted from a three-blade wind turbine satisfies the following cubic law (1.4). The formulas and coefficients used to calculate C_p is (1.5) [7].

$$P_{wind} = \frac{1}{2}\rho_{air}\pi R_{blade}^2 C_p(\beta,\lambda)v_{wind}^3 \quad (1.4)$$

$$\lambda = R_{blade}\frac{w_m}{v_{wind}}$$

$$C_p(\beta,\lambda) = 0.5176\left(\frac{116}{\lambda_i} - 0.4\beta - 5\right)e^{-21/\lambda_i} + 0.0068\lambda \quad (1.5)$$

where ρ_{air} the air density, R_{blade} the blade radius, C_p the aerodynamic coefficient, β the pitch angle, λ the tip speed.

VI. DFIG CONROLLER

Figure 3 shows the control structure of the DFIG wind power generation system. This approach uses vector control to independently regulate the active and reactive power from the grid [8][13][16]. The rotor controller is designed to control the speed of the machine and the stator reactive power. The speed reference is generated by a MPPT algorithm to maximize power generation. The grid controller keeps a constant DC-link voltage regardless of the magnitude or direction of the power flow while ensuring unity power factor at its point of connection.

$$\frac{i_{rdq}}{d_{rdq}} = \frac{V_{DC}}{r_r + L_r\sigma s} \quad (1.6)$$

$$\frac{i_{rdq}}{d_{fdq}} = \frac{V_{DC}}{r_f + L_f s} \quad (1.7)$$

The current transfer function for the RSC is defined by low frequency poles that depend on the passive elements of the induction machine (1.6). The poles at the GSC current transfer function depends on the grid filter parameters (1.7). The gains of the current controllers are calculated using the values listed in Table 1.

Table 1: Calculated PI controllers gains using the Butterworth polynomial [11].

Current Regulators (GSC)	Current Regulators (RSC)
$k_{gp} = \frac{\sqrt{2}\omega_o L - r_g}{v_{dc}\beta}$ $k_{gi} = \frac{\omega_o^2 L}{v_{dc}\beta}$	$k_{Pcr} = \frac{\sqrt{2}w_{owr}\sigma L_r - r_r}{V_{DC}\beta_i}$ $k_{Icr} = \frac{\sigma L_r w_{owr}^2}{V_{DC}\beta_i}$

VII. VALIDATION OF MODEL AGAINST EXPERIMENTAL SETUP

To validate the real-time models, the DFIG model receives the measured grid voltage, the encoder signal, and the emulated rotor voltage. The emulated rotor voltage is calculated by multiplying the PWM signals from the rotor and grid converter by the respective modulation index and DC-Link voltage. The back to back model receives the control signals from the grid and rotor converters, the measured grid voltages, and emulated rotor currents. The aerodynamic and mechanical models were not able to be validated with the testbed.

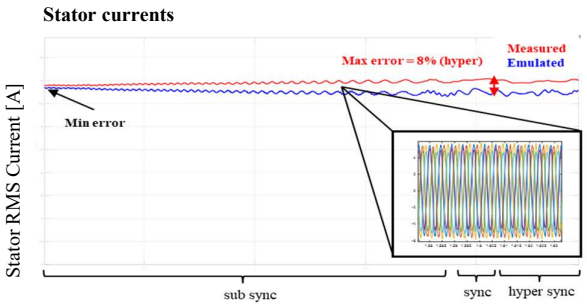

Figure 5: Closed Loop machine model comparison for balanced grid conditions with speed sweep. Red line measured stator current (RMS). Blue line, emulated stator current (RMS).

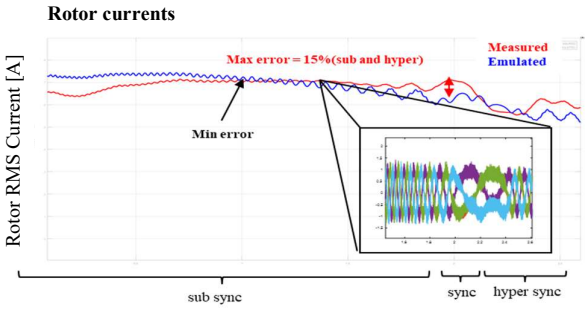

Figure 6: Closed Loop machine model comparison for balanced grid conditions with speed weep. Red line measured rotor current (RMS). Blue line, emulated rotor current (RMS).

The results shown in Figure 5 and Figure 6 were obtained using a closed-loop configuration, where the RSC controls DFIG through subs-synchronous, synchronous and hyper-synchronous speeds. These figures show that the error between the emulated and measured currents varies with the slip. The error for the stator currents is a minimum at sub-synchronous speeds and increases to 8% during hyper-synchronous operation. For the rotor currents, the error is a minimum near the synchronous speed and a maximum at both

sub-synchronous and hyper-synchronous operating points, with an absolute maximum of 15% at 1800 RPM. The difference between the measured and emulated stator and rotor currents warrants further investigation, and as suggested by [1], might be explained by a nonlinear magnetizing inductance whose magnitude is dependent upon the magnitude of the magnetizing current. For reference, the magnetizing inductance of the generator was held constant in the modeling presented here.

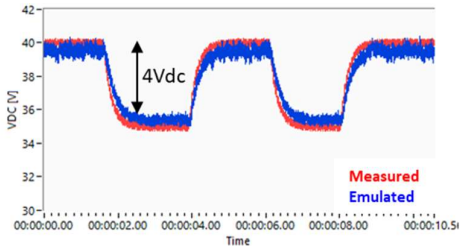

Figure 7: Power electronics model. DC-link voltage reference change.

Figure 7 shows the comparison between the emulated and the measured voltage in the DC-bus. The average model of the back to back inverter executed in real time accurately represents the steady-state values and slow transients, with a steady-state difference between the emulated system and the measurements not exceeding 10% . Future work will strive to address the differences between the DFIG model and the physical DFIG. Concern around space and resource usage on the FPGA is minimal, since most of the FPGA slices are still available, as shown in Figure 8.

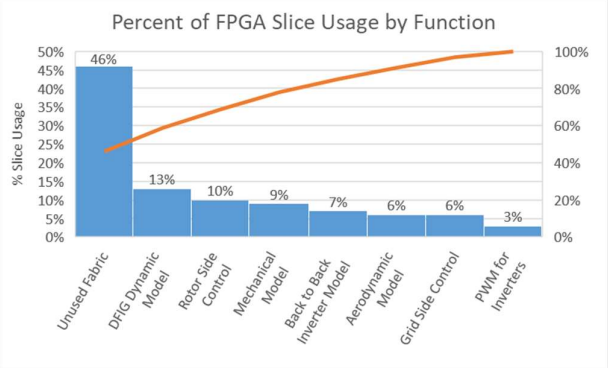

Figure 8: Percent of FPGA slice usage for each model and control scheme.

VIII. REAL TIME EXECUTION OF TYPE-3 WIND TURBINE SYSTEM

The developed Type-3 wind turbine testbed can be executed in PC-layer for offline simulations or can be executed in real-time on the cRIO platform. This section explores the performance difference between these work modes. As expected, both models provide the same results, however the code executed on the PC-layer requires 40m to simulate 35s, while the same code on the FPGA requires 4 minutes to simulate 245 seconds, which is 70 times faster than PC-layer execution, see Figure 9-10.

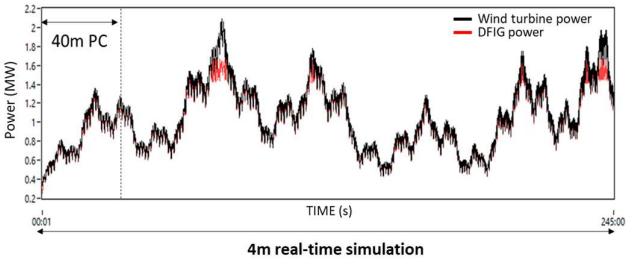

Figure 9: 4 minutes real time simulation .

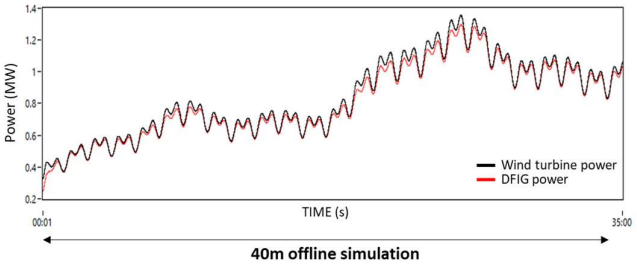

Figure 10: 40 minutes PC-layer simulation.

IX. CONCLUSIONS

This article shows the design and implementation of a real-time simulator for a complete grid-connected Type-3 wind system. The code for the real-time DFIG dynamic models, back to back model, mechanical model, and aerodynamic model were addressed. The dynamic machine model was verified using Hardware in the Loop, where the current signals of the models executed in real time were compared against physical measurements. The closed-loop validation showed that the models provide a good representation of the generator over certain operating speed ranges, with a maximum error of 15% in the rotor currents, and 8% in the stator currents. The ranges of poor representation emphasize the point that models need to be compared against the physical systems they are expected to represent, with an eye towards explaining any discrepancies. Lastly, the developed Type-3 real-time wind emulator runs approximately 70 times faster than the same code executed on the PC-layer, making it an ideal tool to study the low dynamics normally present in wind energy systems.

REFERENCES

[1] Gonzalo Abad, Jesús López, Miguel A. Rodríguez, Luis Marroyo, Grzegorz Iwanski, DOUBLY FED INDUCTION MACHINE MODELING AND CONTROLFOR WIND ENERGY GENERATION, IEEE Press.

[2] C. Dufour and J. Belanger, "Real-time PC-based simulator of electric systems and drives," in *Proc. Int. Conf. Parallel Comput. Elect. Eng.*, Sep. 7–10, 2004, vol. 1, pp. 105–113.

[3] A. Benigni, F. Adler, D. Fetzer, A. Monti and R. DeDoncker, "Real-time simulation of a doubly fed induction generator wind turbine on a new DSP based hardware platform," *2013 15th European Conference on Power Electronics and Applications (EPE)*, Lille, 2013, pp. 1-10.

[4] F. Huerta, R. L. Tello and M. Prodanovic, "Real-Time Power-Hardware-in-the-Loop Implementation of Variable-Speed Wind Turbines," in *IEEE Transactions on Industrial Electronics*, vol. 64, no.

3, pp. 1893-1904, March 2017. doi: 10.1109/TIE.2016.2624259.

[5] V. Dinavahi, M. R. Iravani, and R. Bonert, “Design of a real-time digital simulator for a D-STATCOM system,” *IEEE Trans. Ind. Electron.*, vol. 51, no. 5, pp. 1001–1008, Oct. 2004.

[6] H. Chen, S. Sun, D. C. Aliprantis and J. Zambreno, "Dynamic simulation of DFIG wind turbines on FPGA boards," *2010 Power and Energy Conference At Illinois (PECI)*, Urbana-Champaign, IL, 2010, pp. 39-44.

[7] Lubosny, Zbigniew. WIND TURBINE OPERATION IN ELECTRIC POWER SYSTEMS. 2010. Springer. ISBN 13: 9783540403401

[8] R. Pena, J. C. Clare and G. M. Asher, "Doubly fed induction generator using back-to-back PWM converters and its application to variable-speed wind-energy generation," in *IEE Proceedings - Electric Power Applications*, vol. 143, no. 3, pp. 231-241, May 1996.

[9] M. Ferrari and M. A. Buckner, "Comparison of Doubly-Fed Induction Generator Machine Models for Real-Time Simulations," *2018 9th IEEE International Symposium on Power Electronics for Distributed Generation Systems (PEDG)*, Charlotte, NC, 2018, pp. 1-5. doi: 10.1109/PEDG.2018.8447730

[10] Ferrari Maglia, M. (2012). Análisis, control y operación de turbinas eólicas DFIG en condiciones distorsionadas de red. http://hdl.handle.net/10251/27689.

[11] Bijaya Pokharel. Master thesis. Modeling, Control And Analysis Of A Doubly Fed Induction Generator Based Wind Turbine System With Voltage Regulation

[12] Gonzalo, a. (2008). *Predictive direct control techniques of the doubly fed induction machine for wind energy generation applications*. Ph.d. University of mondragon

[13] D. Zhou, Y. Song and F. Blaabjerg, "Modern control strategies of doubly-fed induction generator based wind turbine system," in *Chinese Journal of Electrical Engineering*, vol. 2, no. 1, pp. 13-23, June 2016

[14] A. Veltman, D. W. J. Pulle, and R.W. De Doncker, Fundamentals of Electric Drives. Springer, 2007..

[15] S. J. Chapman, Electrical Machines. McGraw Hill, 1985

[16] A. Peterson, “Analysis, Modeling and Control of Doubly-Fed Induction Generators for Wind Turbines.” Ph.D. thesis, Chalmers University of Technology, Goteborg, Sweden,

.